

Trigonal manganese cluster in silicon: An electron-paramagnetic-resonance study

J. Kreissl and W. Gehlhoff

Arbeitsgruppe Elektron Paramagnetische Resonanz am Institut für Festkörperphysik, Technische Universität Berlin, Rudower Chaussee 5, D-12484 Berlin, Germany

H. Vollmer

Institut für Angewandte Physik der Technische Universität Clausthal, Arnold-Sommerfeld-Strasse 6, D-38678 Clausthal-Zellerfeld, Germany

(Received 3 November 1993)

Besides the known tetrahedral Mn_4^0 cluster, a second Mn cluster is observed by electron paramagnetic resonance in high-resistivity silicon doped with manganese. The spectrum shows trigonal symmetry. The analysis of the fine structure and the hyperfine structure suggests that the spectrum is due to a cluster consisting of four Mn ions forming a tetrahedron, $[\text{Mn}_{3i}^0\text{-Mn}_i^x]$, where the fourth Mn^x ion gives rise to the trigonal symmetry. Most likely it is either a Mn^- ion at an interstitial site or a Mn^+ ion at a substitutional site. The $[\text{Mn}_{3i}^0\text{-Mn}_i^-]$ cluster model is favored. The observed $S = \frac{11}{2}$ ground-state manifold is the result of the dominant exchange coupling between the electronic spins of the four Mn constituents. The coordination of four ions in a tetrahedron seems to be an energetically preferred state during the formation of bigger clusters in the silicon lattice.

I. INTRODUCTION

Manganese is one of the most extensively studied transition metals (TM's) in silicon and has played an important role for the understanding of TM defects. It is known from the pioneering electron-paramagnetic-resonance (EPR) investigations done by Ludwig and Woodbury¹ that isolated manganese can exist in different charged states, both at interstitial (Mn_i^- , Mn_i^0 , Mn_i^+ , and Mn_i^{2+}) and substitutional (Mn_s^{2-} and Mn_s^+) lattice sites. Furthermore, it is known that manganese forms pairs with other impurities¹⁻⁵ as well as the homonuclear Mn_4^0 cluster.^{1,6,7} To our knowledge, the model developed by Ludwig and Woodbury, which predicts the electronic configurations of TM's, is correct in the case of manganese defects. For a number of manganese and manganese-related defects known from EPR a comprehensive picture has been obtained from space-charge measurements,⁸⁻¹⁰ combined space-charge and EPR investigations,^{6,9,11,12} optical data,^{13,14} and more fundamental theories.^{15,16}

The investigations of the manganese clusters started with the previous EPR studies of Ludwig, Woodbury, and Carlson¹⁷ and Hall-effect measurements done by Carlson.¹⁸ They suggested a cluster model consisting of four manganese atoms at interstitial sites with a total spin $S=2$ and a level position near midgap. During the last decade the investigation of the Mn_4^0 cluster has gained a renewed interest. EPR,⁷ optical,¹² combined EPR and Hall effect,⁶ as well as combined EPR and space-charge measurements¹¹ have been done. The energy level induced by the manganese cluster is still controversially discussed. On the one hand, a level position at midgap^{11,18} and on the other hand a level in the upper half of the gap at $E_c - 0.28$ eV (Ref. 6) have been obtained.

Contrary to that, the nature of the electronic structure seems to be clarified by the detailed EPR investigation given in Ref. 7. The established model, resulting from the analysis of the EPR data, shows that the cluster has tetrahedral symmetry where the four neutral manganese atoms are placed at probably nearest-neighbor interstitial sites forming a regular tetrahedron. In a simple picture the cluster states could be constructed from the electronic states of the single constituents of the cluster as it is usually done in the analysis of EPR spectra of complexes. The local trigonal crystal-field distortion at the Mn_i^0 sites produced in each case by the other three Mn_i^0 atoms partially lifts the orbital degeneracy of the 4T_1 state and causes a 4A orbital singlet ground state. These orbital singlets are coupled by a strong exchange coupling which creates spin multiplets having total spins $S=0, 1, 2, 3, 4, 5,$ and 6 , where the multiplet with $S=6$ is the ground state (ferromagnetic coupling).¹⁹ So far it cannot be decided if the Mn_4^0 cluster is arranged around a substitutional Si site or an interstitial T_d one.²⁰

Concerning the total spin controversy in the literature it should be pointed out that, so far, the observed tetrahedral Mn_4^0 clusters are in all cases the same. This can be demonstrated by the following arguments: (i) The EPR spectra are observed in all cases in high-resistivity starting material where the Mn_4^0 cluster seems to be a preferred manganese center. (ii) We have tested a number of manganese doping procedures with different starting material and various doping and cooling conditions but, so far, when we were able to observe a manganese cluster with cubic symmetry it always showed identical EPR parameters. An experimental hint at another Mn cluster showing the same symmetry does not exist. (iii) The discrepancy of the different hyperfine parameters given in the literature, $A = 12.7 \times 10^{-4} \text{ cm}^{-1}$ (Ref. 1) on the one hand and $A = -13.7 \times 10^{-4} \text{ cm}^{-1}$ (Ref. 7) on the other, can be resolved inferring that in the earlier paper¹ the

sign of A was not determined but was assumed to be positive and, furthermore, that second-order effects in the calculation of line positions were not taken into account increasing the error in extracting the parameter A from the experimental data to about $\pm 1 \times 10^{-4} \text{ cm}^{-1}$. If that most probable imputation is true one attains a coincidence of the hyperfine parameters.

However, there remains the discrepancy between the total spins $S=2$ and 6 in the literature that was attributed to one and the same EPR spectrum. In the earlier papers where the total spin $S=2$ was proposed, neither the angular dependence of the fine structure nor the cubic fine structure parameter " a " has been given. Therefore, the reasons for an assignment of the spectra to $S=2$ cannot be fully appreciated, but we believe that the authors may have overlooked some low-intensity transitions in the angular fine-structure dependence. This led them to estimate a wrong total spin $S=2$.

Recently, calculations of the Fe_4^0 and Mn_4^0 clusters have been published using a molecular silicon cluster model and the multiple-scattering $X\alpha$ theory.²¹ The Fe_4^0 cluster was discovered also by EPR.²² Except for the trigonal symmetry it was described by a model very similar to the one used in the case of the Mn_4^0 cluster.⁷ The four Fe^0 atoms with a spin $S(\text{Fe}_i^0)=1$ are strongly exchange coupled which leads to total spin multiplets of $S=0, 1, 2, 3$, and 4 . Also in this case the coupling is ferromagnetic and for that reason the spin multiplet with $S=4$ is the ground state.

In contrast to the Fe_4^0 cluster where the theory confirms the total spin $S=4$ of the ground state, the results of the calculations on the Mn_4^0 cluster yield $S=0$ for the ground state and are, therefore, incompatible with the EPR data. The authors suggest that the alleged controversial results $S=2$ and 6 are due to excited electronic states originating from several $3d$ -derived impurity levels in the band gap. In our opinion, that conclusion is not valid for the following reasons. First, as described above, there is only one EPR spectrum of a manganese cluster with cubic symmetry that has to be described with a total spin $S=6$ and second, the temperature dependence of the line intensities down to 4 K measured in the dispersion mode of the EPR spectrometer clearly shows that the observed spectrum belongs to the ground state.¹⁹

In a comprehensive investigation by EPR of the first steps toward the formation of larger clusters we have searched for other manganese clusters as well. No experimental or theoretical data on further manganese clusters have been reported so far, except a preliminary observation in Ref. 23. The EPR spectrum which was very briefly reported in that paper is identical to the one discussed here, but in the present paper we show that the guessed Mn_3^0 model given in Ref. 23 is not appropriate for the interpretation of the spectrum. The spectrum shows many lines with a strong angular dependence. The defect will be identified as a new manganese related cluster with trigonal symmetry. The EPR analysis provides strong evidence that the cluster consists of four manganese ions but, in contrast to the known Mn_4^0 , one of them has a different charge state and is possibly moved from the site in a regular tetrahedron.

II. EXPERIMENT

The samples were prepared from several floating-zone and Czochralski-grown silicon crystals by two methods. (i) The manganese doping was performed by encapsulating a small piece of metallic manganese and a carefully etched $\{110\}$ -oriented Si sample in an evacuated quartz ampule. The ampule was heat treated for about 1 h at 1200°C . After the diffusion process the samples were quenched by dropping the ampule into water. To get the highest possible Mn cluster concentration the quenching velocity was varied especially in the high-temperature region. (ii) Manganese was evaporated on the samples in vacuum. The diffusion was carried out in a vertical quartz tube with a silicon sample holder under helium atmosphere. After a rapid quench in diffusion pump oil the specimens showed only the EPR spectrum of interstitial Mn_i^0 . The signal from the cluster grew up within two or four weeks if the samples were kept at room temperature.

The highest concentrations of the Mn clusters were achieved in high-resistivity p -type or n -type material. The EPR measurements in absorption were performed at the X band using a ZWG ERS 230 spectrometer equipped with a fixed-temperature finger cryostat (20.4 K) or a He gas-flow cryostat and in dispersion using a Bruker ESP 200D-SRC equipped with a He gas-flow cryostat for variable temperature measurements. In the case of the fixed-temperature cryostat we used a special goniometer for the *in situ* correction of small misalignments of the crystal.

III. THEORETICAL BACKGROUND: SPIN LEVELS OF A TETRANUCLEAR CLUSTER OF TRIGONAL SYMMETRY IN THE STRONG EXCHANGE LIMIT

The spin Hamiltonian appropriate to describe the EPR spectra of clusters can be written as²⁴

$$\mathcal{H} = \sum_i \mathcal{H}_i + \sum_{i < j} \mathcal{H}_{ij}, \quad i, j = 1, 2, \dots, n, \quad (1)$$

where n is the number of the constituents, \mathcal{H}_i is the spin Hamiltonian of the individual paramagnetic centers, and \mathcal{H}_{ij} the interaction Hamiltonian between them. In the strong exchange limit we deal with a dominant isotropic exchange interaction and consider the effect of other interaction terms as a perturbation. Antisymmetric terms as well as biquadratic and further higher-order terms were omitted.

The most common arrangement of four spins arises from a tetrahedron. In a general arrangement six exchange-coupling constants are needed to describe the magnetic interaction (see Fig. 1). The spin Hamiltonian describing the isotropic exchange interaction between four paramagnetic centers with quenched orbital moments in the ground states takes the form

$$\begin{aligned} \mathcal{H}_{\text{EX}} = & J_{12} S_1 S_2 + J_{13} S_1 S_3 + J_{14} S_1 S_4 \\ & + J_{23} S_2 S_3 + J_{24} S_2 S_4 + J_{34} S_3 S_4. \end{aligned} \quad (2)$$

In a regular tetrahedral geometry as in the case of the known Mn_4^0 cluster all four Mn_i^0 centers are equivalent

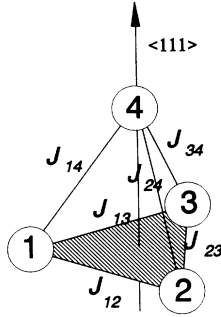


FIG. 1. Exchange-coupling constants for the coupling of four spins.

and of course all coupling constants J_{ij} are equal. In that case, all spin states with the same total spin S are at the same energy.

For the present type of cluster we observed trigonal symmetry, suggesting that two exchange-coupling constants J^* and J^{**} characterize the isotropic exchange interaction with $J^{**}=J_{14}=J_{24}=J_{34}$ and $J^*=J_{12}=J_{23}=J_{13}$. J^* represents the coupling constant within the regular triangle which lies perpendicular to the C_3 symmetry axis and J^{**} characterizes the coupling of the triangle ions to the fourth constituent of the cluster. The spin Hamiltonian appropriate to describe the exchange interaction in this case is

$$\mathcal{H}_{\text{EX}}(C_3) = J^*(S_1 S_2 + S_2 S_3 + S_1 S_3) + J^{**}(S_1 S_4 + S_2 S_4 + S_3 S_4). \quad (3)$$

The eigenvalues of the spin Hamiltonian given in Eq. (3) can be easily found using a coupling scheme described by kets of the form $|S_1 S_2 S_3 S_{123} S_4 S\rangle$, where S_1 to S_4 are the spins of the individual constituents, S_{123} the resulting spins within the regular triangle, and S the spin of the whole cluster. Since $S_{123} = S_1 + S_2 + S_3$ and $S = S_{123} + S_4$ Eq. (3) can be written as

$$\mathcal{H}_{\text{EX}}(C_3) = \frac{1}{2} J^* (S_{123}^2 - S_1^2 - S_2^2 - S_3^2) + \frac{1}{2} J^{**} (S^2 - S_4^2 - S_{123}^2). \quad (4)$$

In the coupling scheme used the energy matrix is diagonal and the eigenvalues are

$$E = \frac{1}{2} J^* \{ S_{123}(S_{123} + 1) - S_1(S_1 + 1) - S_2(S_2 + 1) - S_3(S_3 + 1) \} + \frac{1}{2} J^{**} \{ S(S + 1) - S_4(S_4 + 1) - S_{123}(S_{123} + 1) \}. \quad (5)$$

The experimental data given in Sec. IV suggest a cluster consisting of three equivalent Mn_i^0 atoms arranged in a regular triangle (S_1, S_2, S_3 , with $S_i = \frac{3}{2}$) and one Mn ion with a spin $S_4 = 1$ for the ground states. In the proposed coupling scheme we have 14 different spin states characterized by the following kets $|S_1 S_2 S_3 S_{123} S_4 S\rangle$:

$$\begin{aligned} \{1\} & \left| \frac{3}{2} \frac{3}{2} \frac{3}{2} \frac{9}{2} 1, \frac{11}{2} \right\rangle, & \{2\} & \left| \frac{3}{2} \frac{3}{2} \frac{3}{2} \frac{9}{2} 1, \frac{9}{2} \right\rangle, & \{3\} & \left| \frac{3}{2} \frac{3}{2} \frac{3}{2} \frac{9}{2} 1, \frac{7}{2} \right\rangle, \\ \{4\} & \left| \frac{3}{2} \frac{3}{2} \frac{3}{2} \frac{7}{2} 1, \frac{9}{2} \right\rangle, & \{5\} & \left| \frac{3}{2} \frac{3}{2} \frac{3}{2} \frac{7}{2} 1, \frac{7}{2} \right\rangle, & \{6\} & \left| \frac{3}{2} \frac{3}{2} \frac{3}{2} \frac{7}{2} 1, \frac{5}{2} \right\rangle, \\ \{7\} & \left| \frac{3}{2} \frac{3}{2} \frac{3}{2} \frac{5}{2} 1, \frac{7}{2} \right\rangle, & \{8\} & \left| \frac{3}{2} \frac{3}{2} \frac{3}{2} \frac{5}{2} 1, \frac{5}{2} \right\rangle, & \{9\} & \left| \frac{3}{2} \frac{3}{2} \frac{3}{2} \frac{5}{2} 1, \frac{3}{2} \right\rangle, \\ \{10\} & \left| \frac{3}{2} \frac{3}{2} \frac{3}{2} \frac{3}{2} 1, \frac{5}{2} \right\rangle, & \{11\} & \left| \frac{3}{2} \frac{3}{2} \frac{3}{2} \frac{3}{2} 1, \frac{3}{2} \right\rangle, & \{12\} & \left| \frac{3}{2} \frac{3}{2} \frac{3}{2} \frac{3}{2} 1, \frac{1}{2} \right\rangle, \\ \{13\} & \left| \frac{3}{2} \frac{3}{2} \frac{3}{2} \frac{1}{2} 1, \frac{3}{2} \right\rangle, & \{14\} & \left| \frac{3}{2} \frac{3}{2} \frac{3}{2} \frac{1}{2} 1, \frac{1}{2} \right\rangle. \end{aligned}$$

The reduced energies E/J^* of the spin levels are plotted in Fig. 2 as a function of the ratio J^{**}/J^* . The point at $J^{**}/J^* = 0$ shows the behavior of a regular triangle and the point at $J^{**}/J^* = 1$ corresponds to the case of a regular tetrahedron regarding the coupling constants.

From the dependencies shown in Fig. 2 we can conclude that the experimentally observed $S = \frac{11}{2}$ ground-state manifold occurs if the J^{**}/J^* lies in the range where either both signs of J^{**} and J^* are negative (ferromagnetic coupling) or where $J^{**}/J^* < -4.5$, assuming a positive sign of J^* . In the second case a comparatively small antiferromagnetic coupling in the regular triangle is overcompensated by a strong ferromagnetic coupling of the fourth Mn constituent. Because of the analogy to the tetrahedral Mn_4^0 and Fe_4^0 cluster in silicon the ferromagnetic coupling seems to be most likely (negative coupling constants). In order to analyze the EPR spectra of the exchange-coupled cluster the spin Hamiltonian describing the isotropic exchange interaction given in Eqs. (2)–(4) must be complemented by the terms describing the Zeeman and hyperfine interaction as well as the zero-field splitting of the individual constituents (\mathcal{H}_i) and the anisotropic spin-spin interaction (\mathcal{H}'_{ij}).

$$\mathcal{H}_i = \mu_B B g_i S_i + S_i D_i S_i + \sum_k I^k A^k S_i, \quad (6)$$

$$\mathcal{H}'_{ij} = S_i D_{ij} S_j,$$

where g_i , D_i , D_{ij} , and A_i^k are the g -, zero-field splitting and hyperfine tensors and k runs over all the nuclei with nonzero nuclear spins. In the strong exchange limit the EPR transitions occur only within the sublevels of the total spin S . Therefore, the EPR spectra can be interpreted using spin Hamiltonians for the different total spins S of the form

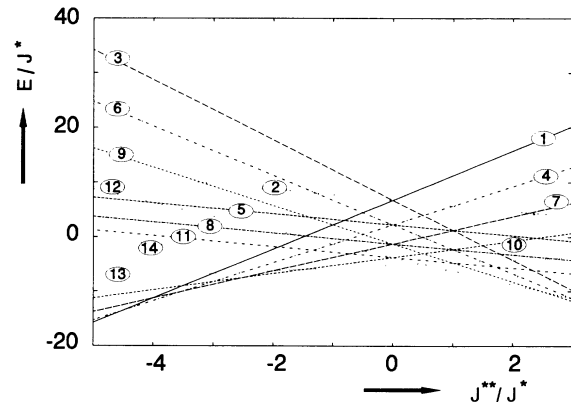


FIG. 2. Dependence of the reduced energies E/J^* for a tetranuclear cluster of trigonal symmetry with three spins of $\frac{3}{2}$ and one spin of 1 on the ratio of the coupling constant J^* characterizing the interaction within the regular triangle to the coupling constant J^{**} , which reflects the coupling of the triangle ions to the fourth constituent. The description of the 14 plotted spin states characterized by the numbers is given in the text.

$$\begin{aligned}\mathcal{H}_S &= \mathcal{H}_{FS} + \mathcal{H}_{HFS}, \\ \mathcal{H}_{FS} &= \mu_B B g_S S + S D_S S, \\ \mathcal{H}_{HFS} &= \sum_k I^k A_S^k S.\end{aligned}\quad (7)$$

The parameters g_S , D_S , and A_S^k can be derived from the parameters of the spin Hamiltonian of the individual constituents, g_i , D_i , and A_i^k , and from those of the anisotropic exchange spin-Hamiltonian D_{ij} (for details see Ref. 24).

IV. EXPERIMENTAL RESULTS AND ANALYSIS

A. Interaction with the crystal field [fine structure]

A strongly angular dependent and many-line EPR spectrum was observed in high-resistivity p -type or n -type silicon samples. In addition to this new spectrum two other Mn-related centers could be observed if the quenching velocity was varied. For faster quenching the well-known isolated Mn_i^0 (Ref. 1) becomes the preferred center in the material. In this case the spectrum discussed in this paper grows during a few days' storage at room temperature. For lower quenching rates, the tetrahedral cluster Mn_4^0 (Refs. 1 and 7) was the preferred one.

The EPR spectra for the main directions ($B \parallel \langle 110 \rangle$, $\langle 111 \rangle$, $\langle 112 \rangle$, and $\langle 100 \rangle$) are shown in Fig. 3. A closer inspection of the structure of the line groups caused by the hyperfine interaction will be given below. Because the fine-structure splitting is large compared to the hyperfine splitting which is evident from the line splittings observed in the spectrum we can separately analyze the fine structure and treat the hyperfine interaction as a perturbation.

The angular dependence of the fine-structure transitions is plotted in Fig. 4. The positions have been estimated as centers of gravity of the hyperfine structures and were taken directly from the experimental plots. The data points were interpolated by continuous lines which coincide with the fitted ones given below and only these are shown in the figure for clarity. The line positions and their intensities depend strongly on the angle between the crystal axes and the magnetic field. Therefore, in many cases the lines cannot be observed for all directions and some lines get out of the magnetic-field limit of our experimental setup which lies between 50 and 1800 mT.

In the following paragraph, we will discuss some essential parts of the angular dependence to evolve an appropriate spin Hamiltonian and to estimate initial values for the computer fit. The behavior around the $\langle 111 \rangle$

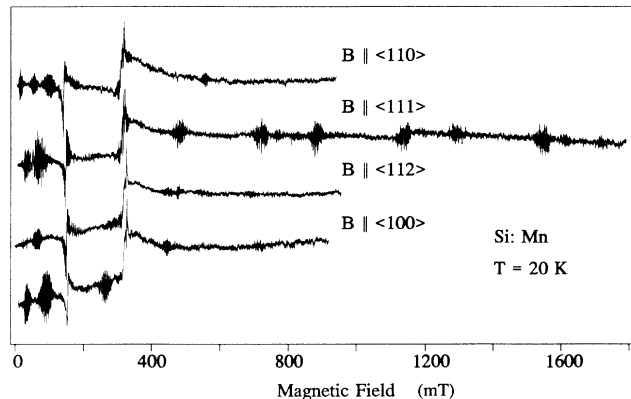


FIG. 3. EPR spectra of the trigonal Mn cluster $[Mn_{3i}^0-Mn_{1j}^0]$ for four main directions. The measurements were performed at $T=20$ K and the microwave frequency was 9.26 GHz. The single, isotropic resonance at $g=2$ is due to the surface signal and the broad step in the spectra near $g=2$ comes from the experimental setup.

direction and parts of the low-field resonance pattern between 50 and 330 mT indicate a trigonal symmetry. A magnified representation of that part of the angular fine-structure dependence is given in Fig. 5. The most intensive groups of transitions occur in the low-field range which is characteristic of a system with an odd number of unpaired electrons in the strong zero-field splitting limit ($D \gg g\mu_B B$). In this limit (assuming a positive D) it is expected that the lowest Kramers doublet is far separated from the other energy levels, so allowed transitions only occur within this doublet. However, the typical pattern of such a behavior could only partially be observed (thicker lines in Fig. 5), because the conditions of a strong zero-field splitting limit are not fulfilled for the whole angular dependence. In the strong zero-field splitting limit the EPR spectrum can be described with an effective spin $S'=1/2$. Assuming $g_{\parallel}=g_{\perp}=2$, the expected effective g' values would be in a first approximation $g'_{\parallel}=2$ and $g'_{\perp}=2S+1$. The experimental g'_{\perp} value could be determined to $g'_{\perp}=9.5(2)$ showing that we have to deal with a half-integral spin system of $S \geq \frac{9}{2}$. As the reason for the experimental deviation of g'_{\perp} from the strong zero-field splitting limits for the possible spins $g'_{\perp}=10$ ($S=\frac{9}{2}$) or 12 ($S=\frac{11}{2}$) and so on we suggest that the electronic Zeeman and zero-field splittings are comparable. This is supported by the fact that the number of transitions (see Fig. 5) exceeds the number of allowed transitions in a $S'=1/2$ system. Neglecting the hyperfine interaction the spin Hamiltonian [Eq. (7)] of such a spin system can be written as²²

$$\begin{aligned}\mathcal{H}_{FS} &= g_{\parallel} \mu_B B_z S_z + g_{\perp} \mu_B (B_x S_x + B_y S_y) + D [S_z^2 - \frac{1}{3} S(S+1)] + \frac{\sqrt{2}}{36} a [S_z (S_+^3 + S_-^3)]_+ \\ &+ \frac{1}{180} (F-a) \{ 35S_z^4 - [30S(S+1) - 25]S_z^2 - 6S(S+1) + 3S^2(S+1)^2 \} \\ &+ \frac{1}{5040} G [\{ 11S_z^3 - [3S(S+1) + 59]S_z \}, (S_+^3 + S_-^3)]_+ \quad \text{with } [A, B]_+ = AB + BA, \end{aligned}\quad (8)$$

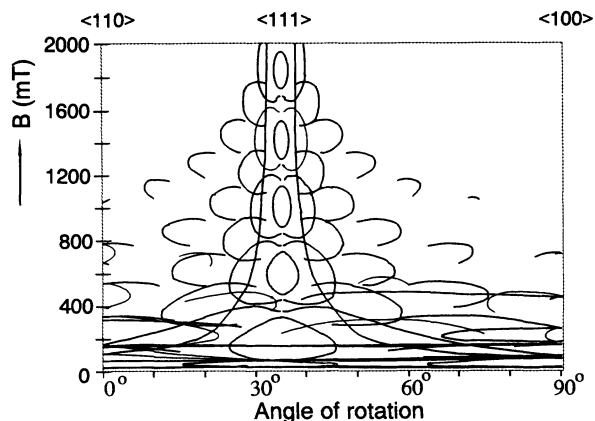


FIG. 4. Angular dependence of fine-structure line positions of the trigonal Mn cluster $[\text{Mn}_{3i}^0-\text{Mn}_i^{\uparrow}]$ obtained at 9.26 GHz. The magnetic field is rotated in a $\{110\}$ crystal plane.

where all symbols have their usual meanings. For the proposed large spin the terms of sixth ($\sim G$) and higher order in S have to be included. However, their influence on the EPR spectra decreases with increasing order. Already the terms containing the parameter a , F , and especially G are not very significant. Therefore, all other possible higher-order terms were neglected in the spin Hamiltonian. The z axis of the coordinate system (x, y, z) coincides with the trigonal C_3 symmetry axis parallel to $\langle 111 \rangle$, and the x and y axes are chosen according to the convention that for centers with $z \parallel [111]$ they are parallel to the $[\bar{1}\bar{1}2]$ and $[1\bar{1}0]$ directions, respectively. Corresponding to the four C_3 directions there are four different center positions, two of which are magnetically equivalent under rotation around a $\langle 110 \rangle$ axis as it was done in our experiment. With the external magnetic field B parallel to the z direction ($\Theta = 0^\circ$) and under the assumption that a and G are small compared with D and/or $g\mu_B B$ which is very likely considering all known Mn-related centers the nondiagonal elements given by the

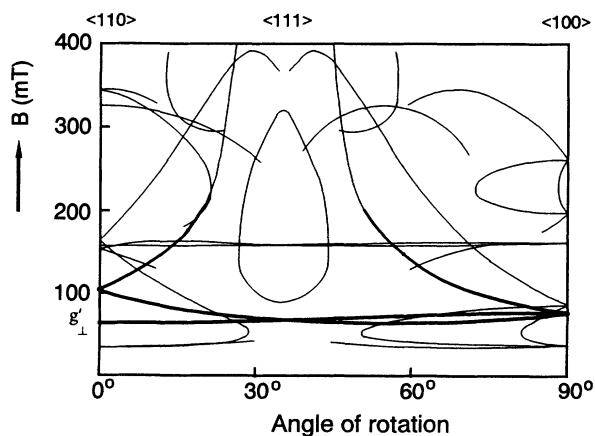


FIG. 5. Part of the angular dependence up to 400 mT of the fine-structure line positions of the trigonal Mn cluster $[\text{Mn}_{3i}^0-\text{Mn}_i^{\uparrow}]$ obtained at 9.26 GHz. The magnetic field is rotated in a $\{110\}$ crystal plane.

terms proportional to a and G can be neglected. In this case, the energy eigenvalues are determined by

$$E(M) = g_{\parallel}\mu_B B M + D[M^2 - \frac{1}{3}S(S+1)] - \frac{a-F}{180} \{35M^4 - [30S(S+1) - 25]M^2 + 3S^2(S+1)^2 - 6S(S+1)\}, \quad (9)$$

where M are the eigenvalues of S_z . Under this condition M is a good quantum number not dependent on the value of D . Therefore, we have only to consider the allowed transitions, i.e., $\Delta M = \pm 1$, in this particular direction. A calculation with a rough set of parameters is helpful to identify those transitions in the $\langle 111 \rangle$ direction of which the C_3 center axis coincide with the direction of the external magnetic field. Using the experimental positions of those transitions the values of the parameters g_{\parallel} , D , and $(a-F)$ were determined from Eq. (9) by a least-square fitting procedure. The result for a guessed spin $S = \frac{1}{2}$ is $g_{\parallel} = 2.06(1)$, $|D| = 0.195(1) \text{ cm}^{-1}$, and $|a-F| = 0.0053(2) \text{ cm}^{-1}$, where the sign of $[D/(a-F)]$ is negative. The corresponding energy levels are shown in Fig. 6(a) together with the allowed $\Delta M = \pm 1$ EPR transitions.

With an arbitrary orientation of the magnetic field the spin Hamiltonian is no longer diagonal, even with neglecting the terms proportional to S^4 and higher orders in S . One way to proceed is to apply perturbation theory but this is not expedient in this case since the trigonal zero-field and the Zeeman splittings are of the same order of magnitude in the region of the magnetic field where the transitions occur. We, therefore, made complete computer diagonalizations of the energy matrix of the spin Hamiltonian (Eq. 8) to calculate the whole angular dependence of the EPR fine-structure line positions and

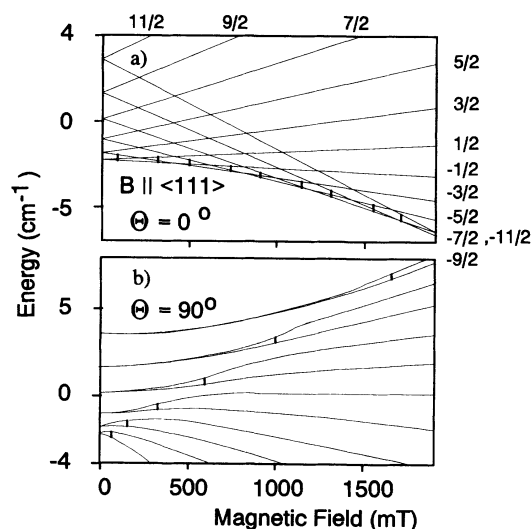


FIG. 6. Energy level diagrams for the $S = \frac{1}{2}$ ground-state manifold of the trigonal Mn cluster for the C_3 axis (a) parallel and (b) perpendicular to the magnetic field. In (a) only the allowed transitions $\Delta M = \pm 1$ have a finite transition probability and are indicated by arrows. In (b) all possible transitions are indicated by arrows but the intensities for the high-field transitions become low.

intensities via the calculation of the eigenvalues and eigenfunctions. An example for a level scheme of an angle where the states are heavily mixed is given in Fig. 6(b) where the C_3 axis of the cluster is perpendicular to the magnetic field ($\Theta=90^\circ$). Furthermore, we tried to fit the calculated rotation pattern to the experimentally observed one. The coinciding rotation patterns are shown in Figs. 4 and 5. Those transitions have been dropped where the intensity is smaller than $\frac{1}{10}$ of the largest intensity calculated for the whole angular dependence. The parameters of the spin Hamiltonian that give the best fit are summarized in Table I.

In the following we will discuss the determination of the spin $S = \frac{11}{2}$. It is already known from the preliminary discussion given above that we have to deal with a half-integral spin system $S \geq \frac{9}{2}$. For this reason we have calculated the angular fine-structure dependence around the $[111]$ direction ($\pm 5^\circ$) for that center which has its trigonal axis parallel to the $[111]$ direction. The results for the two spins $S = \frac{9}{2}$ and $\frac{11}{2}$ are given in Fig. 7. In both plots the experimentally determined line positions of the allowed fine-structure transitions $\Delta M = \pm 1$ were included by open circles for $B \parallel z$. Though the upper limit of our magnetic field is at 1800 mT it can clearly be seen that the high-field point cannot be explained with a spin $S = \frac{9}{2}$, therefore, such a spin can be ruled out. Contrary to that the calculation with $S = \frac{11}{2}$ is in agreement with the experimental points which have already been used for the fitting of the parameters g_{\parallel} , D , and $(a-F)$ given above. The validity of a spin higher than $\frac{11}{2}$ cannot be ruled out by the discussed behavior around the direction $B \parallel z$ because (i) we were not able to measure all allowed transitions on account of the magnetic-field limit of our experimental setup and (ii) the fitting of the "egg"-shaped pattern in the realized magnetic-field range does not depend essentially on the used spin for $S \geq \frac{11}{2}$. Taking into account only the terms of the Zeeman interaction and the zero-field splitting proportional to D the "egg" diameters in the $\langle 111 \rangle$ direction are independent on the spin for $S \geq \frac{11}{2}$ and equal to $2(B_0 - D')$ with $B_0 = h\nu / (g_{\parallel} \mu_B)$ (D' indicates that the value D is given in mT units). The consideration of further terms proportional to $(a-F)$ and higher than fourth order should give a spin-dependent contribution to the "egg" diameters. However, those contributions might be used for a final decision of the spin but in the present case the contributions are too small compared to the experimental errors of the line positions.

A decision regarding the spin requires one to take into

TABLE I. Data of the spin Hamiltonian of the trigonal Mn cluster: $[\text{Mn}_{3i}^0 - \text{Mn}_1^{\uparrow}]$.

S	$\frac{11}{2}$
g_{\parallel}	2.06(1)
g_{\perp}	2.00(2)
$ D $	0.195(1) cm^{-1}
$ a-F $	0.0053(2) cm^{-1}
$\text{sgn}[D/(a-F)]$	negative
$A(\text{Mn}_3)$	$21(2) \times 10^{-4} \text{cm}^{-1}$
$A_{\parallel}(\text{Mn}_1)$	$\approx 39 \times 10^{-4} \text{cm}^{-1}$

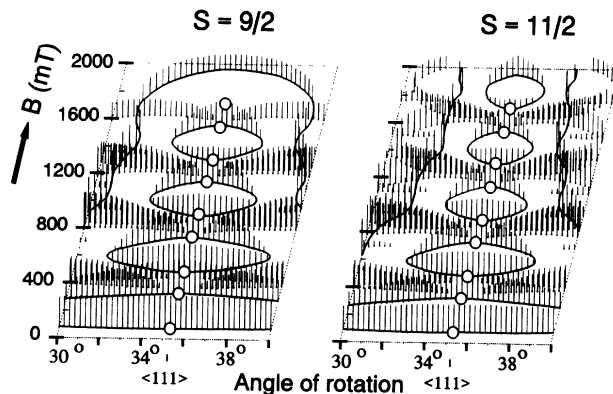


FIG. 7. Comparison of the calculated angular fine structure dependencies around the direction $C_3 \parallel B$ for $S = \frac{9}{2}$ (left) and $S = \frac{11}{2}$ (right) with the experimentally observed values given by circles. The calculated transition probabilities are indicated by the stick lengths of the vertical bars that are attached to the calculated points. Points were dropped completely if the intensities are smaller than $\frac{1}{10}$ of the largest intensities. The interpretation is given in the text.

consideration further experimental data of the fine-structure rotation pattern, and last but not least the fitting of the whole angular dependence. But for illustration the comparison of the experimental g'_{\perp} -value and the estimated $g'_{\perp}(S)$ values will be useful. Because perturbation theory up to second order for the calculation of $g'_{\perp}(S)$ in the strong zero-field limit is not sufficient for our system we calculate the $g'_{\perp}(S)$ values using the magnetic-field value for the transition $M = \frac{1}{2}$ to $M' = -\frac{1}{2}$ achieved by the computer diagonalization of the energy matrix for $B \perp z$ using the parameters given in Table I (except the spin S which is used as a variable). In dependence of the spin $S = \frac{9}{2}, \frac{11}{2},$ and $\frac{13}{2}$ we obtain the following calculated values $g'_{\perp}(S)$: (i) $g'_{\perp}(\frac{9}{2}) = 8.46$, (ii) $g'_{\perp}(\frac{11}{2}) = 9.43$, (iii) $g'_{\perp}(\frac{13}{2}) = 11.78$, which have to be compared with the experimentally determined value $g'_{\perp} = 9.5(2)$. It can be seen that only the calculated $g'_{\perp}(\frac{11}{2})$ value coincides with the experimental data. Therefore, all other spins higher than $\frac{11}{2}$ can be ruled out and we conclude that the spin $S = \frac{11}{2}$ is the only one which satisfies the observed fine structure. The seemingly arbitrary choice of the real g_{\perp} value which only allows a comparison of the experimental and calculated g'_{\perp} values is confirmed by the achieved good coincidence of the experimental and calculated line positions and intensities for the whole angular dependence of the fine-structure transitions. The g values near 2 support that assumption of an orbital singlet ground state for the observed cluster.

The dependence of the intensity of the EPR spectrum on temperature shows whether the $S = \frac{11}{2}$ state is the ground state or not. For these measurements the EPR spectrometer was tuned to the dispersion mode because the absorption spectra are strongly saturation at temperatures below 20 K. The results are shown in Fig. 8. The experimental data given in Fig. 8 by closed circles reflect the population of the observed cluster state derived from the EPR intensity and they are compared with the

theoretical temperature dependence following the Boltzmann population of the different spin multiplets S which are given by lines. The level scheme for the used parameters of the isotropic exchange coupling is calculated using Eq. (5) and is shown in the inset of Fig. 8. The level population given in Fig. 8 is derived from the experimentally observed intensity dependence in the following manner. Since for simplicity it can be assumed that the microwave conditions of the system, the line shape, and linewidth remain unchanged during the variation of the temperature the line intensity is proportional to two temperature dependent terms. One of them is the population probability of a level i related to a ground level 0 which we are looking for and the second one reflects the population difference between the two Zeeman levels where the EPR transition occurs. The second term $(1 - e^{-(h\nu/kT)})$ is known for a given microwave frequency and temperature. Therefore, we calculate the thermal population of the cluster levels dividing the measured intensities by the second factor. However, a good fit of the experimental values can only be achieved if the $S = \frac{11}{2}$ manifold is the lowest-lying level, e.g. the ground state (the further splitting of the $S = \frac{11}{2}$ manifold is small compared to the exchange splitting and, therefore, they can be omitted in this discussion here). It has to be repeated here that the J^* and J^{**} exchange parameters given for the fit in Fig. 8 are only one possible set because an unambiguous determination is not possible as long as excited spin states cannot be observed. But the temperature dependence of the ground-state population allows us to estimate an energy distance of about 20 cm^{-1} to the first excited level.

The analysis of the fine-structure behavior has doubtless given the result that the EPR spectra are produced by a ground-state multiplet with $S = \frac{11}{2}$ in a trigonal distorted tetrahedral crystal field. In a preliminary discussion we conclude that the cluster consists of four constit-

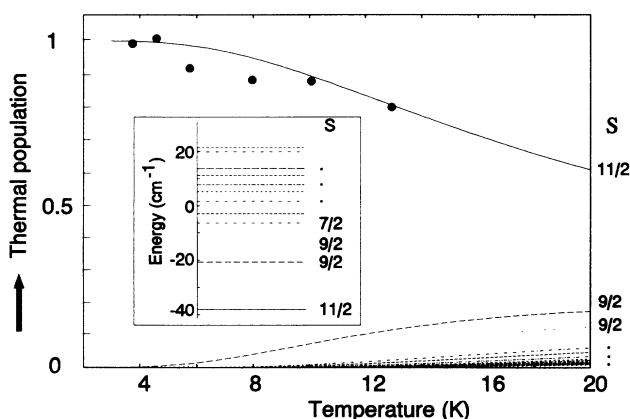


FIG. 8. Experimental and calculated temperature dependence of the population of the cluster levels. The experimental points were derived as one part of the measured EPR intensities of the transition $M = \frac{1}{2}$ to $M' = -\frac{1}{2}$ for $C_3||B$ and they are drawn by closed circles. The calculated curves present the normalized thermal population according to the level scheme given in the inset. The parameters $J^{**} = -4 \text{ cm}^{-1}$ and $J^* = -3 \text{ cm}^{-1}$ used here are one possible set of exchange-coupling parameters that satisfies the experimental points.

uents forming an axial distorted tetrahedron. It is most probably that the total spin $S = \frac{11}{2}$ is built up by a strong exchange coupling between three Mn_i^0 atoms with an effective spin $S(\text{Mn}_i^0) = \frac{3}{2}$ and a fourth one Mn^x with an effective spin $S(\text{Mn}^x) = 1$. The charge state and the site of the last one will be discussed below.

The spectrum of the trigonal cluster could be observed in the dark as well as under illumination with band gap or below band-gap light. We were not able to prove any influence of the light. It should be pointed out here that also in samples containing both types of clusters, the tetrahedral Mn_4^0 and the trigonal cluster, we were not able to convert one to the other by illumination.

B. Interaction with nuclear spins of the cluster constituents [hyperfine (HF) interaction]

It is well known that the analysis of the HF structure is the best tool for identifying the constituents of a paramagnetic defect. But in the present case of a cluster we are not able to give a quantitative analysis of the whole angular dependence of the observed HF structures. The reasons for these difficulties are that we have to deal with only partially resolved, extremely angular dependent structures and a comparatively low signal-to-noise ratio because of the occurrence of a many-line spectrum. Furthermore, for arbitrary directions a simultaneous occurrence of allowed and forbidden nuclear-spin transitions is expected and, moreover, in many cases the HF structures belonging to different fine-structure transitions are superimposed. In the following, we try to give a qualitative analysis for some selected HF structures.

For most of the HF structures a line distance of about 2.2 mT is characteristic. Moreover, a distribution of HF intensities could be more or less clearly observed, which is typical for an isotropic HF interaction of a homonuclear pair or a small cluster where the constituents have isotopes with a nonzero nuclear spin and a high natural abundance. An example for such a structure is shown in Fig. 9(a). The large number of HF transitions indicates that the constituents of the cluster must have a large nuclear spin. Intrinsic defects can be excluded because the silicon isotope with a nuclear spin ^{29}Si has only a natural abundance of 4.7% and a nuclear spin $I = \frac{1}{2}$. From the behavior that the spectrum occurs only in manganese-doped silicon, from the order of magnitude of the hyperfine splitting, from the large number of HF lines requiring a large nuclear spin, and from intensity considerations—about 10^{15} – 10^{16} atoms/cm³ must contribute to the observed intensity of the spectrum—manganese with a nuclear spin $I = \frac{5}{2}$ and a natural isotope abundance of 100% is the only candidate that can be responsible for observed EPR spectrum supporting the assumptions of a four Mn cluster made in Sec. IV A.

As already mentioned above, a first estimation shows that the strength of the HF interaction is about two orders of magnitude smaller than the Zeeman and zero-field splittings. Therefore, the part of the HF interaction of the Hamiltonian given in Eq. (7),

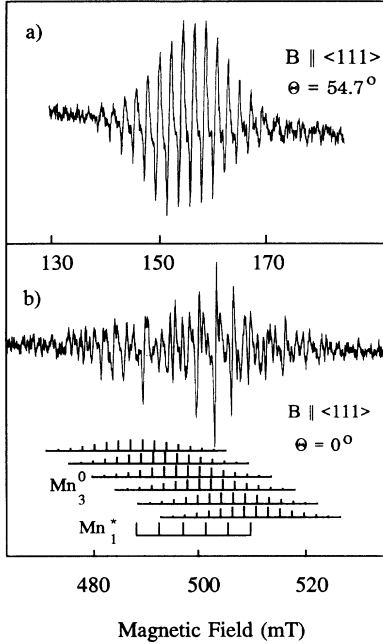


FIG. 9. Hyperfine structures of two electronic-spin transitions for $B \parallel \langle 111 \rangle$ at 20 K belonging (a) to the centers whose angles between the magnetic field and the z axes are $\Theta = 54.7^\circ$ and (b) to the $M = -\frac{3}{2}$ to $M' = -\frac{1}{2}$ transition for $z \parallel B$ ($\Theta = 0^\circ$). The allowed $\Delta m = 0$ nuclear-spin transitions are represented by the stick spectra for the four Mn ions.

$$\mathcal{H}_{\text{HFS}} = \sum_{k=1}^4 (A_{x'_k}^k S_{x'_k} I_{x'_k}^k + A_{y'_k}^k S_{y'_k} I_{y'_k}^k + A_{z'_k}^k S_{z'_k} I_{z'_k}^k), \quad (10)$$

can be treated as a perturbation. Index k relates to the cluster constituents, each of which has its own system of principal axes x'_k, y'_k, z'_k for the HF interaction. The analysis of the fine-structure behavior has already given the result that we are dealing with a cluster of trigonal symmetry probably consisting of four manganese constituents. For that reason it seems to be convenient to assume that the three equivalent Mn ions have C_{3h} symmetry at the site of the nucleus. The principal values of the HF tensor are equal for the three equivalent Mn ions. Whereas trigonal symmetry is expected for the fourth particular Mn ion placed on the axis of the trigonal distortion, the principal HF axes x'_4, y'_4, z'_4 coincide with the principal axes of the fine structure (x, y, z).

The HF structure and the estimation of some components of the HF tensors should be considerably simplified for orientations where the C_3 symmetry axis of the cluster defect is parallel to the external magnetic field since only allowed nuclear-spin transitions should occur. In Fig. 9(b) the observed HF structure for the electronic-spin transition $M = -\frac{1}{2}$ to $M' = -\frac{3}{2}$ is shown where the C_3 symmetry axis of the cluster is parallel to the magnetic field. But in the presented case of a cluster the HF structure becomes not very simple. We try to explain this HF structure within the model discussed above. For an orientation $C_3 \parallel B$ one expects a line scheme representing

the splitting due to one particular Mn ion placed on the C_3 axis and to three equivalent Mn ions [see stick spectra in Fig. 9(b)]. The particular Mn ion produces the well-known six line structure which is further split by the three equivalent Mn ions. The HF structure of three equivalent Mn ions consists of 16 lines with a distribution of intensities 1:3:6:10:15:21:25:27:25:... In Fig. 9(b) the attempt of a qualitative explanation of the observed HF structure is given by the calculated stick spectrum using the following HF parameters: $A(\text{Mn}_3) = 2.2$ mT and $A_{\parallel}(\text{Mn}_1) = 4.1$ mT.

It seems that the HF structure of the interaction with the three Mn ions placed in a plane perpendicular to the C_3 axis has only a weak angular dependence because nearly the same line distance is found for nearly all structures as mentioned above [see, for example, Fig. 9(a)] and, therefore, the HF parameters for the three Mn ions are assumed to be isotropic with a value of about $A(\text{Mn}_3) = 2.2$ mT. The estimation of the HF parameter of the particular ion, $A_{\parallel}(\text{Mn}_1)$, has a comparatively large uncertainty. This parameter is estimated mainly from the whole width of the HF structure which can be influenced by the occurrence of a forbidden transition due to very small misalignments. Therefore, the value $A_{\parallel}(\text{Mn}_1)$ obtained from the fit may be too large. The occurrence of allowed and forbidden nuclear-spin transitions is due to a strong mixing of nuclear states. Such a behavior was extensively studied in the case of the MnB pair in silicon³ and was also observed in the cases of MnIn and MnGa.^{4,5} Especially around the $\langle 111 \rangle$ direction, the HF structures are extremely sensitive to misalignments. In spite of our special goniometer for an *in situ* correction of small misalignments of the crystal which allows to reduce the misalignment of an axis below 0.2 degree we were not able to reproduce the HF structures in each detail.

Even though the achieved level of the analysis of the HF structures by itself does not allow us to give an unambiguous identification of the cluster defect, the incorporation of manganese has been clearly demonstrated and the model of a Mn cluster of four Mn arranged as a tetrahedron is supported.

V. DISCUSSION

The EPR spectrum discussed in this paper has been discovered in high-resistivity n -type as well as p -type silicon doped with manganese. The angular dependence of the fine structure has been argued to be determined by the general features of an orbital singlet with an electronic spin $S = \frac{1}{2}$ in a trigonal distorted crystal field. The assumption of an orbital singlet is supported by the g values determined to be near 2. The trigonal zero-field splitting and the Zeeman energy at the EPR transitions are of the same order of magnitude, and we are, therefore, faced with a so-called intermediate case leading to some closed curves in the angular dependence and strongly angular dependent transition probabilities of allowed and forbidden transitions. The temperature dependence of the line intensities shows that the observed spectrum reflects the ground state of the defect.

Each fine-structure transition is further split in many lines by the hyperfine interaction. The explanation of the hyperfine structure for some orientations supports the model that the defect is caused by a cluster defect consisting of four manganese ions where one of them is a particular one. Because of this particular manganese ion we are dealing with the behavior of a heteronuclear cluster although all constituents of the cluster are manganese ions.

The Mn cluster is assumed to consist mainly of neutral Mn atoms placed on interstitial sites, since the cluster only occurs in high-resistivity silicon in which the isolated interstitial Mn is found to be in the neutral charge state and because equally charged ions feel a repulsive Coulomb interaction that would prohibit the cluster formation. So far we know that Mn ions occupying a substitutional site appear only in silicon samples that contain in addition large concentrations of Ag or Cu.^{1,2,9} The occurrence of substitutional manganese was also supposed in highly *P*-doped silicon as well as in intrinsic material at sufficiently low diffusion temperatures between 700 and 850 °C.²⁵ Both conditions do not apply to our samples.

We therefore propose the following model of the defect: It is most likely that the cluster consists of four manganese forming a tetrahedron with trigonal symmetry. The reason for the trigonal distortion should be the particular fourth manganese ion. It has been argued that the spin $S = \frac{11}{2}$ is the result of a strongly exchange-coupled manganese cluster named $[\text{Mn}_{3i}^0\text{-Mn}_i^x]$ where the coupling is ferromagnetic. At the site of each constituent the symmetry is lowered by the other constituents, so the orbital moments of the ground states are quenched. As in the case of the cubic Mn_4^0 cluster the cluster spin states were composed assuming for each interstitial Mn_i^0 ($3d^7$) an 4A orbital singlet ground state [$S(\text{Mn}_i^0) = \frac{3}{2}$] in account of the monoclinic symmetry at the interstitial Mn_i^0 sites (C_{1h}) and a spin $S = 1$ for the fourth particular manganese ion feeling trigonal symmetry (C_{3h}). The resulting 14 spin multiplets of $S = \frac{1}{2}, \frac{3}{2}, \dots, \frac{11}{2}$ are given in Sec. III.

The charge state and the site of the fourth particular manganese ion cannot be determined unambiguously yet, but according to the model of Ludwig and Woodbury¹ an interstitial Mn_i^- ion ($3d^8$) with an 3A ground state or a substitutional Mn_s^+ ion ($3d^2 + 4$ binding electrons) also with an 3A ground state are the most likely candidates because of their $S = 1$ ground-state manifolds. The isotropic g values of both isolated defects are about 2.1.¹ Using the usual ionic description the cluster can be described either by a negatively charged cluster $[\text{Mn}_{3i}^0\text{-Mn}_i^-]$ or a positively charged one $[\text{Mn}_{3i}^0\text{-Mn}_s^+]$ depending on the fourth manganese ion. It should be repeated that neither the isolated Mn_i^- nor the isolated Mn_s^+ could be observed even in those samples where the agglomeration process had not been finished and the EPR spectrum of isolated Mn_i^0 was also registered. From the literature we know the level positions of the isolated centers $\text{Mn}_i^-/\text{Mn}_i^0$ at $E_c - 0.12$ eV,⁸ $\text{Mn}_i^0/\text{Mn}_i^+$ at $E_c - 0.46$,^{8,11} and $\text{Mn}_s^0/\text{Mn}_s^+$ at $E_v + 0.39$ eV.⁹ This indicates that the Fermi level lies in the upper half of the gap but below $E_c - 0.12$ eV. Since we have not observed

any signal of charged isolated Mn centers in our samples the charging of the one particular cluster atom must happen during the clustering process connected with the participation of at least one additional defect center. The nature of this center is still unknown for we could not find any further EPR signal.

The formation of the $[\text{Mn}_{3i}^0\text{-Mn}_s^+]$ cluster should be only possible if an interstitial Mn undergoes a transition to a substitutional site during the clustering process leading to a silicon self-interstitial. According to the diffusion of Au in silicon²⁶ the diffusion of these self-interstitials to the sample surface is very slow, so this could not explain the growth of the cluster within a few days at room temperature. For our crystals to be free from dislocations the only possibility to explain the relatively large clustering rate is that some further clusters act as sinks for the self-interstitials. This cannot be excluded, therefore, we cannot rule out the $[\text{Mn}_{3i}^0\text{-Mn}_s^+]$ model although we favor the easier formation mechanism of the $[\text{Mn}_{3i}^0\text{-Mn}_i^-]$ cluster, where all ions occupy interstitial sites.

So far we assumed tacitly that the observed ground state of the cluster reflects the highest spin state as is expected for a strong isotropic exchange interaction where the spin coupling is ferromagnetic. In our opinion, the ferromagnetic coupling is most probable because of the analogy to the similar Mn_4^0 and Fe_4^0 clusters in silicon where a ferromagnetic coupling was reported.^{7,22} But it remains uncertain whether the ground state is not the highest spin state in the case of a deviation from a pure ferromagnetic coupling (see Fig. 2) or in the case of perceptible contributions of biquadratic, anisotropic, and antisymmetric terms in the spin Hamiltonian of the exchange interaction.²⁴ If that would happen, the Mn charge states, Mn_i^+ ($3d^6$) and Mn_s^- ($3d^4 + 4$ binding electrons), which could have an integer spin greater than one in low symmetry, could not be ruled out as candidates for the fourth particular ion.

Two possible geometrical nearest-neighbor arrangements of the proposed cluster defect are shown in Fig. 10, where the Mn ions are placed in (a) around an interstitial site and in (b) around a substitutional site. The three possible geometrical arrangements given in Fig. 10(a) and 10(b) where the Mn^x is placed on an interstitial site fulfill the conditions for the favored model of the negative $[\text{Mn}_{3i}^0\text{-Mn}_i^-]$ cluster. By the EPR results alone one cannot decide between these and other positions of the fourth particular Mn ion shifted along the C_3 axis (indicated by the arrows in Fig. 10), but the large parallel HF parameter $A_{\parallel}(\text{Mn}_1) = 4.1$ mT lying in the order of magnitude of the isolated manganese centers supports the assumption that the fourth Mn ion is placed on the nearest interstitial site with respect to the three neutral Mn atoms in the triangle. In Fig. 10(b) where the Mn^x is placed on a substitutional site the possibility of the geometrical arrangement of the positive $[\text{Mn}_{3i}^0\text{-Mn}_s^+]$ cluster model is demonstrated.

So far two Mn clusters, each consisting of four constituents, have been observed, a neutral cubic one, $[\text{Mn}_4^0]^0$, and a negative trigonal one, $[\text{Mn}_{3i}^0\text{-Mn}_i^-]^-$. The appear-

ance of their spectra can be explained by either the existence of two independent cluster configurations or the observation of two charge states of one defect. In the latter case the charging must be accompanied by a lattice relaxation lowering the overall symmetry of the cluster from cubic to trigonal. The negatively charged state of the cubic cluster without a lattice relaxation should keep the cubic symmetry and change only the total spins. The lattice relaxation might be realized by an off-center position of the fourth particular Mn ion or a jump of this ion to the empty interstitial site at the center of the regular tetrahedron. At the low temperatures during the EPR measurements this geometrical relaxation might be energetically prohibited giving an argument for the missing photoinduced recharging.

Summarizing the discussion given above and keeping in mind all remaining uncertainties the discovered EPR spectrum is most probably caused by a $[\text{Mn}_{3i}^0-\text{Mn}_i^-]$ cluster where the Mn_i^- ion occupies the interstitial site in the center of the regular tetrahedron [Fig. 10(a)].

In the following we will discuss briefly why other possible interpretations of the EPR spectrum are unlikely or can be ruled out.

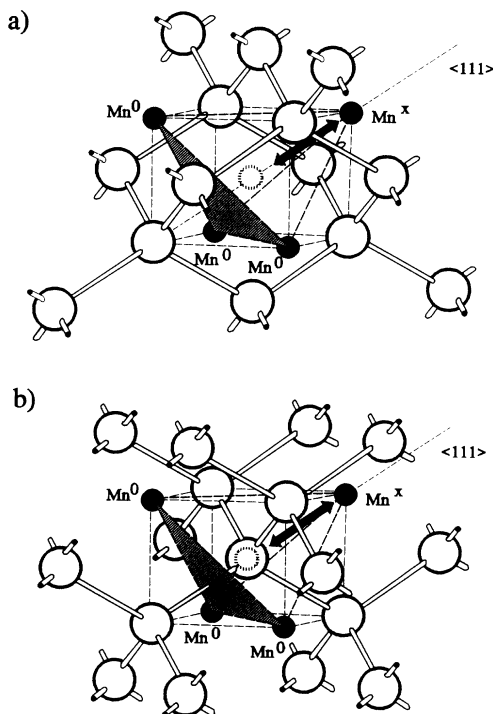


FIG. 10. Proposed structural models for the trigonal Mn cluster $[\text{Mn}_{3i}^0-\text{Mn}_i^-]$ in the silicon lattice, where the Mn ions are placed around (a) a tetrahedral interstitial site or (b) a substitutional site. The double arrows should indicate that in the case of the particular fourth ion Mn^x our data do not allow us to decide between shifted positions on the trigonal axis. The two possible high-symmetric sites are represented by closed and open circles. A description of the possible charge states and sites of the fourth particular Mn ion Mn^x is given in the text. As a result of the discussion the $[\text{Mn}_{3i}^0-\text{Mn}_i^-]$ model is favored where the Mn_i^- is placed on the center of the regular tetrahedron.

(1) Homonuclear pairs and triples

Both kinds of cluster defects can be ruled out. Pairs of manganese on arbitrary sites and charge states can never achieve a $S = \frac{11}{2}$ spin state. Triples can form a triangle of equal ions perpendicular to the $\langle 111 \rangle$ direction or build up a row in $\langle 111 \rangle$ direction leading to trigonal symmetry in both cases. The given analysis of the HF structure can rule out these possibilities and additionally in the case of the recommended regular triangle the spin $S = \frac{11}{2}$ cannot be achieved by three Mn_i^0 atoms.

(2) Larger clusters $n > 4$

For clusters with five or more constituents an unresolved HF structure would be expected because the number of HF transitions increases whereas the line distances decrease.

(3) Heteronuclear clusters

We cannot absolutely exclude the possibility that additional defects take part satisfying the observed trigonal symmetry and hyperfine structure, but the EPR spectra could be explained alone with manganese constituents as it was described above.

During the agglomeration of manganese to precipitations the tetrahedral arrangement of four manganese atoms with predominant neutral constituents (Mn_4^0 or $[\text{Mn}_{3i}^0-\text{Mn}_i^x]$) is a preferred and stable state. So far pairs or triples could never be observed. For low-resistivity starting material where the isolated manganese defects are charged we were not able to identify any homonuclear Mn cluster. The reason might be the repulsive Coulomb force.

VI. CONCLUSIONS

The analysis of the EPR spectra of high-resistivity Si:Mn samples has evidenced a further Mn cluster, $[\text{Mn}_{3i}^0-\text{Mn}_i^x]$, besides the two other known Mn-related defects in this type of material, the isolated Mn_i^0 and the cubic Mn_4^0 cluster. The Mn cluster described in this paper has trigonal symmetry. The interpretation of the hyperfine structure and the determined electronic spin $S = \frac{11}{2}$ for the observed spectrum let us conclude that the cluster consists of four Mn ions forming a distorted tetrahedron, where three of them are equivalent Mn_i^0 ions on interstitial sites with a $S(\text{Mn}_i^0) = \frac{3}{2}$ ground-state manifold. The fourth Mn ion, Mn^x , is a particular one with a spin $S(\text{Mn}^x) = 1$. It is most probable that this fourth Mn ion is a Mn^- ion on an interstitial site or a Mn^+ ion on a substitutional site. The usual incorporation of manganese on interstitial sites favors the $[\text{Mn}_{3i}^0-\text{Mn}_i^-]$ model where the Mn_i^- probably occupies the center of a regular tetrahedron. The particular fourth ion is the reason for the trigonal symmetry of the cluster. The $\frac{11}{2}$ ground-

state manifold of the cluster can be understood in a picture of a dominant isotropic exchange interaction between the electronic spins of the cluster constituents by a ferromagnetic coupling. Because pairs or triples could not be observed the tetrahedral coordination of neutral transition metals seems to be an energetically preferred step in the formation of bigger clusters.

ACKNOWLEDGMENTS

The authors are greatly indebted to R. Labusch, K. Irmischer, and H. Overhof for many useful comments and I. Gründler for technical assistance. We would like to thank U. Rehse for his support in the computer calculations.

-
- ¹G. W. Ludwig and H. H. Woodbury, in *Solid State Physics*, edited by F. Seitz and D. Turnbull (Academic, New York, 1962), Vol. 13, p. 223.
- ²H. Dietrich, H. Vollmer, and R. Labusch, *Solid State Commun.* **58**, 811 (1986).
- ³J. Kreissl and W. Gehlhoff, *Phys. Status Solidi B* **112**, 695 (1982).
- ⁴J. Kreissl, W. Gehlhoff, P. Omling, and P. Emanuelsson, *Phys. Rev. B* **42**, 1731 (1990).
- ⁵J. Kreissl, K. Irmischer, W. Gehlhoff, P. Omling, and P. Emanuelsson, *Phys. Rev. B* **44**, 3678 (1991).
- ⁶H. Feichtinger and R. Czaputa, in *Proceedings of the Satellite Symposium to ESSDERC '82 Munich on Aggregation Phenomena of Point Defects in Silicon*, edited by E. Sirtl and J. Gorrissen (The Electrochemical Society, Electronic Division, Pennington, 1982), Vol. 83-84, p. 134.
- ⁷J. Kreissl and W. Gehlhoff, *Phys. Status Solidi B* **145**, 609 (1988).
- ⁸H. Lemke, *Phys. Status Solidi A* **64**, 549 (1981); **76**, 223 (1983).
- ⁹M. Heider, H. Sitter, R. Czaputa, H. Feichtinger, and J. Oswald, *J. Appl. Phys.* **62**, 3785 (1987).
- ¹⁰H. Feichtinger, J. Oswald, R. Czaputa, P. Vogel, and K. Wüstel, in *Proceedings of the 13th International Conference on Defects in Semiconductors*, edited by L. C. Kimerling and J. M. Parsey, Jr. (The Metallurgical Society of AIME, New York, 1984), Vol. 14a, p. 855.
- ¹¹K. P. Abdurakhmanov, A. A. Lebedev, J. Kreissl, and Sh. B. Utamuradova, *Fiz. Tekh. Poluprovodn.* **19**, 213 (1985) [*Sov. Phys. Semicond.* **19**, 133 (1985)].
- ¹²K. Irmischer and J. Kreissl, *Phys. Status Solidi A* **116**, 755 (1989).
- ¹³H. Conzelmann, *Appl. Phys. A* **42**, 1 (1987).
- ¹⁴T. Bever, P. Emanuelsson, M. Kleverman, and H. G. Grimmeiss, *Appl. Phys. Lett.* **55**, 254 (1989).
- ¹⁵A. Zunger, in *Solid State Physics*, edited by H. Ehrenreich, F. Seitz, and D. Turnbull (Academic, New York, 1986), Vol. 39, p. 275.
- ¹⁶F. Beeler, O. K. Anderson, and M. Scheffler, *Phys. Rev. B* **41**, 1603 (1990).
- ¹⁷G. W. Ludwig, H. H. Woodbury, and R. O. Carlson, *J. Phys. Chem. Solids* **8**, 490 (1959).
- ¹⁸R. O. Carlson, *Phys. Rev.* **104**, 937 (1956).
- ¹⁹Because of the strongly saturated EPR absorption spectra of the Mn_4^0 below 20 K we were not able to prove the ground-state behavior of the $S=6$ spectra by measuring the temperature dependence of the intensities at temperatures below 20 K in Ref. 7. Now we are able to turn the spectrometer to dispersion and the measurements of the temperature dependence of the intensity of the $S=6$ spectra shows clearly that the $S=6$ spin multiplet is the lowest one, e.g., the ground state.
- ²⁰Note that in Ref. 7 only the possibility of a Mn cluster around a substitutional site is discussed due to a mistake.
- ²¹J. R. Leite, L. V. C. Assali, and A. T. Lino, *Mater. Sci. Forum* **83-87**, 221 (1992).
- ²²S. H. Muller, G. M. Tuynman, E. G. Sieverts, and C. A. J. Ammerlaan, *Phys. Rev. B* **25**, 25 (1982).
- ²³J. Kreissl, A. A. Lebedev, and Sh. B. Utamuradova, in *Proceedings of the 7th International School on Defects in Crystals*, Szczyrk, 1985, edited by E. Mizera (World Scientific, Singapore, 1987), p. 264; M. Holst, Diplomawork, Clausthal, 1990.
- ²⁴A. Bencini and D. Gatteschi, *EPR of Exchange Coupled Systems* (Springer-Verlag, Berlin, 1990).
- ²⁵D. Gilles, W. Schröter, and W. Bergholz, *Phys. Rev. B* **41**, 5770 (1991).
- ²⁶N. A. Stolwijk, B. Schuster, J. Hölzl, H. Mehrer, and W. Frank, *Physica* **116B**, 335 (1983).